J Chin Med Assoc

ORIGINAL ARTICLE

POFUT1 promotes gastric cancer progression through Notch/Wnt dual signaling pathways dependent on the parafibromin-NICD1-β-catenin complex

Shuang Dong[a], Zhirong Wang[b,*], Wujun Xiong[c,*]

[a]Center for Single-Cell Omics, School of Public Health, Shanghai Jiaotong University School of Medicine, Shanghai, China; [b]Department of Gastroenterology, Shanghai Tongji Hospital Affiliated to Tongji University, Shanghai, China; [c]Department of Gastroenterology, Shanghai Pudong Hospital, Fudan University Pudong Medical Center, Shanghai, China

Abstract

Background: Aberrant glycosylation performed by glycosyltransferases is a leading cause of gastric cancer (GC). Protein O-fucosyltransferase 1 (POFUT1) expression is increased in GC specimens and cells. In this study, the biological effects and mechanisms of POFUT1 underlying the development of GC were investigated.

Methods: POFUT1 downregulated and upregulated GC cells were established. The effects of POFUT1 on cell proliferation, metastasis and apoptosis were examined using cell counting kit-8 (CCK8) assay, transwell assay, and flow cytometry. Subcutaneous xenograft tumor models were established followed by immunohistochemistry staining of resected tumors. Facilitating modulators and transcription factors were detected by western blot, immunofluorescence, luciferase reporter assay, and co-immunoprecipitation.

Results: POFUT1 played a pro-oncogenic role both in vivo and in vitro, which promoted proliferation and metastasis, as well as inhibited apoptosis in GC cells. POFUT1 promoted Cyclin D3 expression and inhibited the expression of apoptotic proteins, such as Bcl-2-associated X protein (Bax) and cleaved caspase 3, facilitating tumor growth. Moreover, POFUT1 accelerated matrix metalloproteases expression and attenuated E-cadherin expression, contributing to GC metastasis. In addition, POFUT1 expression promoted the expression and nuclear translocation of Notch1 intracellular domain (NICD1) and β-catenin and inhibited β-catenin phosphorylation degradation, accompanied by the activation of recombination signal binding protein-Jκ (RBP-J) and T-cell factor (TCF) transcription factors, respectively. It is notable that parafibromin integrated NICD1 and β-catenin, enabling the concerted activation of Wnt and Notch signaling targeted proteins.

Conclusion: These observations indicated that POFUT1 promoted GC development through activation of Notch and Wnt signaling pathways, which depended on the parafibromin-NICD1-β-catenin complex. This work provides new evidence for the further diagnosis and treatment of GC.

Keywords: Gastric cancer; Notch signaling; Protein O-fucosyltransferase 1; Wnt signaling

1. INTRODUCTION

Gastric cancer (GC) is one of the most common cancers, although a steady decline in incidence and mortality has been observed more recently.[1] The rate of early diagnosis is low; therefore, most patients who are at an advanced stage may miss the best surgical window. Despite the development of immunotherapy and molecular targeted therapies,[2] GC remains essentially an intractable disease. Identification of effective targets may be of great help in controlling GC progression.

Glycosylation catalyzed by glycosyltransferases (GTs) is the most frequent and structurally complex post-translational modification that occurs on the cell surface and secreted proteins. Aberrant glycosylation favors malignant phenotypes and contributes to poor GC outcomes.[3] O-fucosylation, a special type of fucosylation, plays various roles in cellular events and is of great significance to Notch signaling.[4] Protein O-fucosyltransferase 1 (POFUT1) glycosylates epidermal growth factor-like (EGF) repeats within the consensus sequence Cys^2X_{4-5}-Ser/Thr-Cys3 (X represents any amino acid) by adding O-fucose to serine/threonine.[5,6] It has been reported that POFUT1 participates in modulating the stability of EGF repeats and cooperates with protein O-glucosyltransferase 1 (POGLUT1) to fold and trigger the notch receptors to activate notch signaling.[7,8] Previous studies have demonstrated a functional association between POFUT1 and tumorigenesis in oral cancer,[9] hepatocellular carcinoma,[10] breast cancer,[11] lung cancer,[12] and myeloid leukemia.[13] POFUT1 regulates lymphoid and myeloid homeostasis

*Address correspondence. Dr. Zhirong Wang, Department of Gastroenterology, Shanghai Tongji Hospital Affiliated to Tongji University, 389, Xincun Road, Putuo District, Shanghai, China. E-mail address: wangzr929@126.com (Z. Wang); Dr Wujun Xiong, Department of Gastroenterology, Shanghai Pudong Hospital, Fudan University Pudong Medical Center, 2800, Gongwei Road, Pudong New District, Shanghai, China. E-mail address: xiongwujun@126.com (W. Xiong).

Conflicts of interest: The authors declare that they have no conflicts of interest related to the subject matter or materials discussed in this article.

Journal of Chinese Medical Association. (2023) 86: 806-817.

Received December 31, 2022; accepted April 11, 2023.

doi: 10.1097/JCMA.0000000000000957.

through modulation of Notch receptor ligand interactions.[14] Additionally, the POFUT1 variant in humans causes global developmental delay, presenting as microcephaly with vascular and cardiac defects,[15] and Dowling-Degos disease.[16,17] Our findings revealed that POFUT1 expression was increased in GC patients and associated with aggressive tumor phenotypes, as well as with poor differentiation.[18] However, the effect and mechanism of POFUT1 in modulating GC progression are still unknown.

Notch signaling is a highly conserved signaling pathway in metazoan organisms and its dysregulation may lead to multiple diseases and disorders. Whether Notch signaling acts as a suppressive or pro-oncogenic driver depends on the cellular context.[19] Additionally, Wnt signaling is another important pathway that plays a major role in various biological processes, such as embryonic stem-cell development, tissue regeneration, cell differentiation, and immune cell regulation.[20] Nevertheless, little is known about the interaction between Notch and Wnt signaling in GC.

Consequently, investigation of the contribution and related mechanism of POFUT1 in GC development were urgently required. Furthermore, we studied the downstream effects of POFUT1 and crosstalk between Notch and Wnt signaling pathways.

2. METHODS

2.1. Cell culture

Human GC cell lines (HGC-27, MGC-803, BGC-823, SGC-7901, AGS, and MKN-28) and human gastric epithelial cell line (GES-1) were obtained from the cell bank of the Chinese Academy of Sciences (Shanghai, China). Cells were cultured in 90% Roswell Park Memorial Institute 1640 (RPMI-1640, Gibco, Grand Island, NY, USA) or Dulbecco's modified Eagle's medium (DMEM, Gibco) medium supplemented with 10% fetal bovine serum (FBS) and 100 U/mL penicillin and streptomycin (Gibco) at 37°C in a humidified incubator with 5% CO_2.

2.2. Quantitative real-time polymerase chain reaction

POFUT1 messenger RNA (mRNA) expression was detected in GC cells using quantitative real-time polymerase chain reaction (q-PCR). Cells were treated with TRIzol reagent (Invitrogen, Carlsbad, CA, USA) for RNA extraction. Complementary DNA (cDNA) was synthesized using an RT-PCR kit (TaKaRa, Tokyo, Japan) and amplified using q-PCR, according to the protocol of the SYBR q-PCR Kit (Toyobo, Osaka, Japan) using a Roche LightCycler 480 thermal cycler (Roche, Basel, Switzerland). The primers used were as follows: POFUT1: 5′-AACCAGGCCGATCACTTCTTG-3′ (forward); 5′-GTTGGTGAAAGGAGGCTTGTG-3′ (reverse); glyceraldehyde-3-phosphate dehydrogenase (GAPDH): 5′-GGAGCGAGATCCCTCCAAAAT-3′ (forward); 5′-GGCTGTTGTCATACTTCTCATGG-3′ (reverse). Gene transcripts were normalized to GAPDH and the relative fold change was calculated using the $2^{-\Delta\Delta CT}$ method.

2.3. Western blot analysis

Cells were incubated in a radioimmunoprecipitation assay (RIPA) lysis buffer (Beyotime, Nanjing, China), a cocktail (Sigma, Germany) of protease and phosphatase inhibitors (Roche Applied Science, Mannheim, Germany) for 1 hour and 30 minutes at 4°C. Protein lysates were centrifuged at 12 000 × *g* for 20 minutes at 4°C, and protein supernatant concentrations were detected using Pierce bicinchoninic acid (BCA) protein assay kit (Thermo Scientific, Carlsbad, CA, USA). Equal cell lysates were clarified using appropriate sodium dodecyl sulphate polyacrylamide gel electrophoresis (SDS-PAGE) gels for 1 hour at 20 mA. The proteins were transferred electrophoretically to nitrocellulose membranes, which were blocked with tris buffered saline (TBS) (50 mM Tris, 150 mM NaCl, pH 7.6) and supplemented with 0.1% Tween-20 (TBST) containing 5% fat-free dry milk at room temperature. The membranes were then incubated with the specific primary antibodies according to the recommended dilution. After washing with TBST, the membranes were incubated with the secondary antibodies and then visualized using an electrochemiluminescence (ECL) detection system. The specific antibodies used were as follows: POFUT1 (ab74302, Abcam, Cambridge, United Kingdom), HES1 (ab71559, Abcam), actin (ab179467, Abcam), GAPDH (ab181602, Abcam), Notch1 (4380S, Cell Signaling Technology, Boston, MA, USA), p-β-catenin (Ser33/37/Thr41, 9561S, Cell Signaling Technology), cleaved caspase 3 (9664T, Cell Signaling Technology), anti-mouse IgG-horseradish peroxidase (HRP) (No. 7076, Cell Signaling Technology), anti-rabbit IgG-HRP (No. 7074, Cell Signaling Technology), hemagglutinin (HA; No. 5017, Cell Signaling Technology), Myc (No. 2276, Cell Signaling Technology), Flag (No. 14793, Cell Signaling Technology), β-catenin (66379-1-Ig, Proteintech, Chicago, IL, USA), Cyclin D3 (26755-1-AP, Proteintech), matrix metalloproteinase 3 (MMP3; 17873-1-AP, Proteintech), MMP7 (10374-2-AP, Proteintech), E-cadherin (20874-1-AP, Proteintech), and Bcl-2-associated X protein (Bax; 50599-2-Ig, Proteintech). The results were representative of at least three independent experiments and analyzed quantitatively using ImageJ software (National Institutes of Health, Bethesda, MD, USA).

2.4. Transfection and stable clone selection

MGC-803 and BGC-823 cells were chosen for transfection and stable clone selection. Specific plasmids and lentivirus transduction were supplied by Shanghai Asia-Vector Biotechnology Co., Ltd (Shanghai, China). The cDNAs encoding human POFUT1, Notch1 intracellular domain (NICD1), β-catenin, and parafibromin were cloned into the pcDNA3 vector (Invitrogen). Stable cell lines were selected using a puromycin treatment after transfection, and then validated using western blotting.

2.5. CCK8 assay

Three thousand cells were cultured in 96-well plates for 1 to 6 days. After the addition of a cell counting kit-8 (CCK8) solution mixed with DMEM, cells were incubated for 1 h and the absorbance was measured at 450 nm using an EnVision microplate reader (PerkinElmer, MA, USA). All experiments were performed in triplicates.

2.6. Apoptosis assay

Apoptosis assays were performed using an Annexin V PE Apoptosis kit (BD Biosciences, San Jose, CA, USA) and flow cytometry. Cells were seeded into dishes and then treated according to the manufacturer's instructions.

2.7. Cell migration and invasion transwell assays

The treated cells were suspended in serum-free medium and then seeded into the upper chambers of a transwell (8 μm, 24-well insert) at a density of 1.0×10^5 cells per well. The upper chambers with or without Matrigel matrix (BD Biosciences) were used for cell migration and invasion assays. The cells in the lower chamber containing 20% FBS were observed after incubation for 48 hours. As cells in the upper chambers were removed, cells in the lower chambers were fixed with ethanol,

and then stained with 5% crystal violet. Eight random fields of the remaining cells were photographed and counted under a microscope.

2.8. Immunofluorescence staining

Cells were washed with phosphate buffer solution and fixed with 4% paraformaldehyde at 4°C for 15 minutes. The cells were then permeabilized with 0.1% Triton X-100 and incubated with specific primary antibodies overnight. Nuclei were stained with 4',6-diamidino-2-phenylindole (DAPI). Images were viewed using a laser confocal microscopy system (Leica Sp5 laser scanning confocal microscope; Wetzlar, Germany).

2.9. Immunohistochemistry

Paraffin-embedded tissue slides from a nude mice subcutaneous xenograft tumor model were dewaxed and rehydrated. After the endogenous peroxidase was blocked, the slides were blocked with bovine serum albumin and then incubated with the primary antibodies specific for Ki67 and cleaved caspase 3. Slides were incubated in biotinylated secondary antibodies and streptavidin-peroxidase conjugate at 37°C. Then 3,3′-diaminobenzidine was added as a chromogen substrate. Images were viewed using a microscope system (Olympus, Tokyo, Japan).

2.10. Subcutaneous xenograft tumor model

The animal study was approved by the Medical Ethics Committee to observe tumor transplantation and formation in vivo. BGC-823 cells stably transfected with lentiviral particles were implanted subcutaneously into 6-week-old nude mice and then monitored for tumor growth. All mice were sacrificed 6 weeks later. Tumor sizes were evaluated using the following equation: $V = L \times W^2/2$ (L = long diameter; W = wide diameter) and assessed using immunohistochemistry (IHC).

2.11. Luciferase reporter assay

The 3′ untranslated region of recombination signal binding protein-Jκ (RBP-J) was amplified using genomic DNA and primers (forward: 5′-CTATCGATAGGTACCCAGGAAGCCT CCCCGGCGCG-3′; reverse: 5′-CGGAATGCCAAGCTTCCC CGCCGCCTTTCCCTGCT-3′) containing KpnI and HindIII restriction sites. The primers used for T-cell factor (TCF) amplification were 5′-TAGCCCGGGCTCGAGAGCAGAGCT GGGGTCGCTTG-3′ (forward) and 5′-GGGCTGGGAGAC GGCTGGACAAGCTTGGCATTCCG-3′ (reverse). The PCR products were ligated to luciferase reporter vectors (pGL3 vector). Luciferase activity was tested using the dual luciferase reporter assay kit (Promega, Fitchburg, WI, USA) according to the manufacturer's protocol. The results were obtained from triplicate samples from three independent experiments.

2.12. Co-immunoprecipitation

Cells were treated with Nonidet P-40 cell lysis buffer. The acquired cell lysates were incubated with the respective antibodies and protein G-beads (GE Healthcare, Chicago, USA). The beads were then washed six times with a lysis buffer, and the immune complex was eluted using an SDS-PAGE sample buffer.

2.13. Statistics

The quantitative data were obtained from at least three samples, and the values are expressed as mean ± SD. Statistical analyses were carried out using SPSS software version 17.0 (IBM Inc., Chicago, IL, USA). Data analyses were performed using either a two-tailed unpaired Student's *t* test or one-way analysis of variance (ANOVA). A $p < 0.05$ was considered statistically significant.

3. RESULTS

3.1. Knockdown of POFUT1 inhibits the proliferation and metastasis but accelerates the apoptosis of GC cells

POFUT1 is highly expressed in GC specimens. To investigate POFUT1 expression in GC cells, we detected POFUT1 expression in human gastric epithelium cells (GES-1) and six GC cell lines (HGC-27, MGC-803, BGC-823, SGC-7901, AGS, and MKN-28). A high POFUT1 expression was observed in six GC cells in different degrees at the mRNA and protein levels (Fig. 1A). Among these cells, MGC-803, SGC-7901, AGS, and MKN-28 exhibited relatively high POFUT1 expression, while BGC-823 and HGC-27 shared relatively low POFUT1 expression. MGC-803 and BGC-823 cell lines that showed highest and lowest POFUT1 expression were chosen for further in vitro studies, in which cells were transfected with lentivirus containing short hairpin RNAs (shRNA) targeting POFUT1 (shPOFUT1) or lentivirus containing scramble nonsense control shRNA (shNC). The knockdown efficiency of POFUT1 was confirmed using western blotting. Quantitative results are shown in Figure 1B. The CCK8 assay was performed to test cell growth capacity, and the results showed that POFUT1 knockdown significantly inhibited cell growth viability relative to the negative control in both MGC-803 and BGC-823 cells (Fig. 1C). Cell growth inhibition rates of MGC-803 on day 6 were 24.86% ± 2% (shPOFU1-1) and 30.01% ± 3% (shPOFUT1-2). Cell growth inhibition rates of BGC-823 on day 6 were 25.53% ± 1% (shPOFU1-1) and 28.79% ± 3% (shPOFUT1-2). Transwell assays were used to detect the migratory and invasive abilities of POFUT1-silenced GC cells. As shown in Figure 1d, the low expression of POFUT1 in MGC-803 and BGC-823 cells led to poor migratory and invasive abilities compared to the negative control. Then, cell apoptosis was investigated using cytometry by using Annexin V and 7-Aminoactinomycin D (7-AAD) staining of MGC-803 and BGC-823 cells. Compared to the control, POFUT1-silenced MGC-803 and BGC-823 cells showed higher percentages of cells undergoing apoptosis (Fig. 1E).

3.2. Notch signaling inhibitor DAPT reverses the carcinogenesis of POFUT1 overexpression

To further verify participation of POFUT1 and Notch signaling in GC development, GC cells overexpressing POFUT1 were established and then treated with γ-secretase inhibitor DAPT (N-[N-(3, 5-difluorophenacetyl)-l-alanyl]-s-phenylglycinet-butyl ester) (10 μM for 72 hours) which specifically inhibits the Notch signaling pathway. As shown in Fig. 2A, the protein levels of POFUT1 were significantly increased in MGC-803 and BGC-823 cells overexpressing POFUT1 compared to those in control and vector-transfected cells. The CCK8 assay revealed that MGC-803 and BGC-823 cells with POFUT1 upregulation showed higher cell growth relative to control and vector-transfected cells, whereas DAPT-treated GC cells with and without POFUT1 upregulation exhibited lower cell growth relative to vector-transfected and POFUT1 upregulated cells (Fig. 2B). Transwell assays indicated that POFUT1 overexpression promoted the migratory and invasive ability of MGC-803 and BGC-823 cells, while DAPT treatment attenuated the pro-migration and pro-invasion effects (Fig. 2C). Regarding the analysis of cell apoptosis, POFUT1 overexpressing cells showed a slightly decreased apoptotic rate compared to that in control and vector-transfected cells, while the cells incubated with DAPT showed a markedly enhanced apoptotic rate to varying degrees. DAPT-incubated MGC-803 and BGC-823 cells with an upregulation of POFUT1 presented a median apoptotic rate (Fig. 2D).

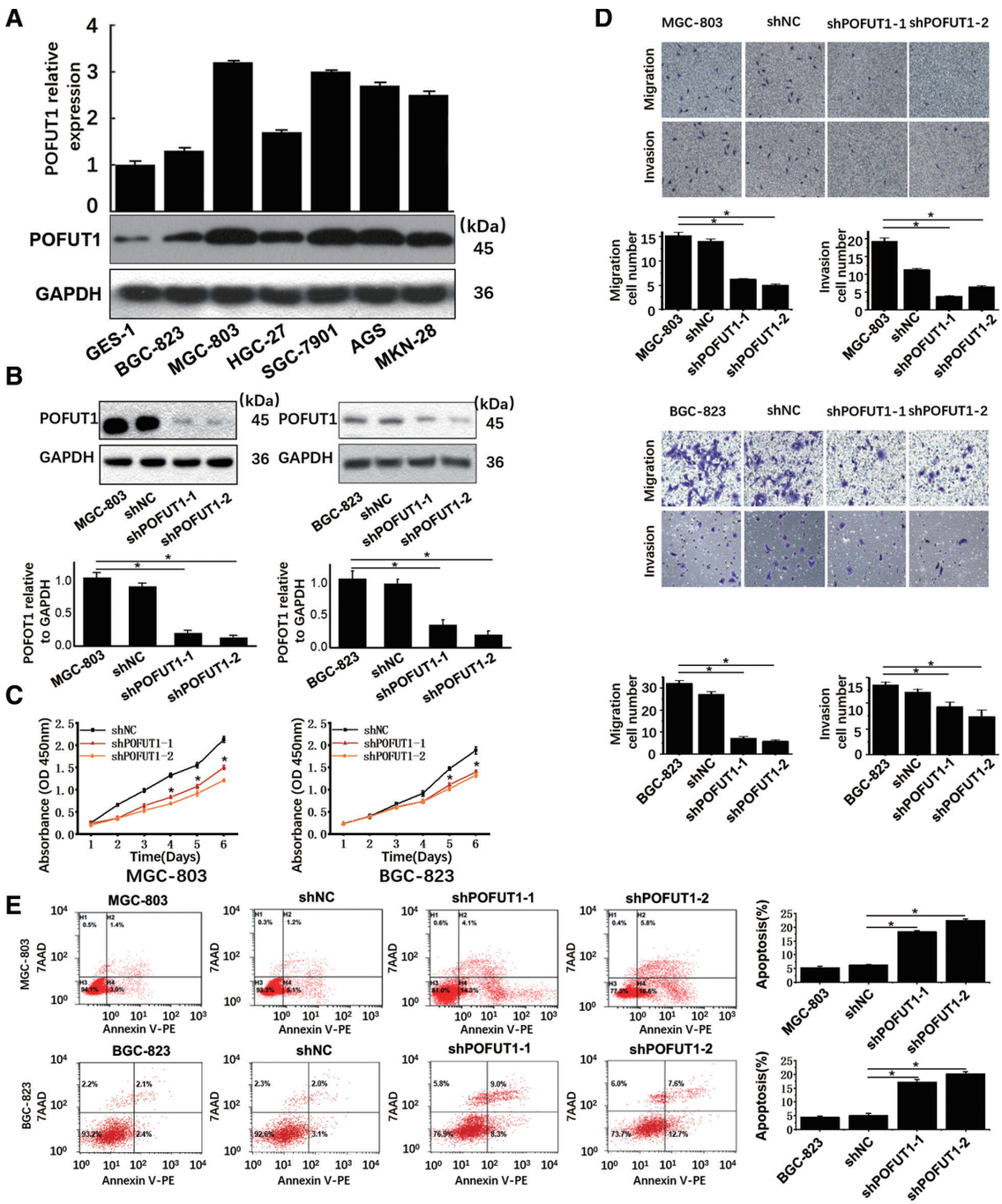

Fig. 1 The expression and knockdown effects of POFUT1 in GC cells. A, mRNA levels (top panel) and protein levels (bottom panel) of POFUT1 in human GES-1 and six GC cell lines. GAPDH was used as a loading control. B, MGC-803 and BGC-823 cell lines were, respectively, transfected with lentiviral shNC, shPOFUT1-1, or shPOFUT1-2. POFUT1 knockdown efficiency was tested using western blotting and analyzed quantitatively as follows ($p < 0.001$): 81.13% ± 19% (MGC-803 shPOFUT1-1); 87.45% ± 12% (MGC-803 shPOFUT1-2); 67.14% ± 32% (BGC-823 shPOFUT1-1); 80.01% ± 19% (BGC-823 shPOFUT1-2). C, Cell growth curves of MGC-803 (left panel; red line: $p = 0.011$ [4 days]; $p = 0.002$ [5 days]; $p < 0.001$ [6 days]; orange line: $p = 0.017$ [4 days]; $p = 0.002$ [5 days]; $p < 0.001$ [6 days]) and BGC-823 cells (right panel; red line: $p = 0.003$ [5 days]; $p = 0.001$ [6 days]; orange line: $p = 0.004$ [5 days]; $p < 0.001$ [6 days]). D, Cell migration and invasion results of POFUT1-silenced MGC-803 cells (top panel; left figure $^*p = 0.022$ and $p = 0.017$; right figure $^*p = 0.014$ and $p = 0.041$) and BGC-823 cells (bottom panel; left figure $^*p = 0.012$ and $p = 0.005$; right figure $^*p = 0.01$ and $p = 0.004$) using transwell assays. Representative images of penetrated cells are shown. Magnification: ×100. Inhibition rate for migratory abilities in MGC-803 cells were 68.9% ± 3% (shPOFUT1-1) and 79.94% ± 5% (shPOFUT1-2). Inhibition rate for invasive abilities in MGC-803 cells were 76.01% ± 3% (shPOFUT1-1) and 57.89% ± 2% (shPOFUT1-2). Inhibition rate for migratory abilities in BGC-823 cells were 77.92% ± 3% (shPOFUT1-1) and 82.19% ± 4% (shPOFUT1-2). Inhibition rate for invasive abilities in BGC-823 cells were 31.62% ± 6% (shPOFUT1-1) and 45.36% ± 7% (shPOFUT1-2). E, Cell apoptosis analysis of POFUT1-silenced MGC-803 (top panel; $^*p = 0.004$ and $p = 0.003$) and BGC-823 (bottom panel; $^*p = 0.019$ and $p = 0.013$) cells using flow cytometry. Results are shown as the mean ± SD based on triplicate experiments using a bar graph. $^*p < 0.05$. AGS, BGC-823, HGC-27, MGC-803, MKN-28, SGC-7901 = human gastric cancer cell lines; 7-AAD = 7-Aminoactinomycin D; Annexin V-PE = annexin V-PE apoptosis detection kit; GAPDH = glyceraldehyde-3-phosphate dehydrogenase; GC = gastric cancer; GES = gastric epithelium cell; GES-1 = human gastric epithelial cell line; mRNA = messenger RNA; POFUT1 = protein O-fucosyltransferase 1; shNC = lentivirus containing scramble nonsense control shRNA; shPOFUT1 = lentivirus containing short hairpin RNAs (shRNA) targeting POFUT1.

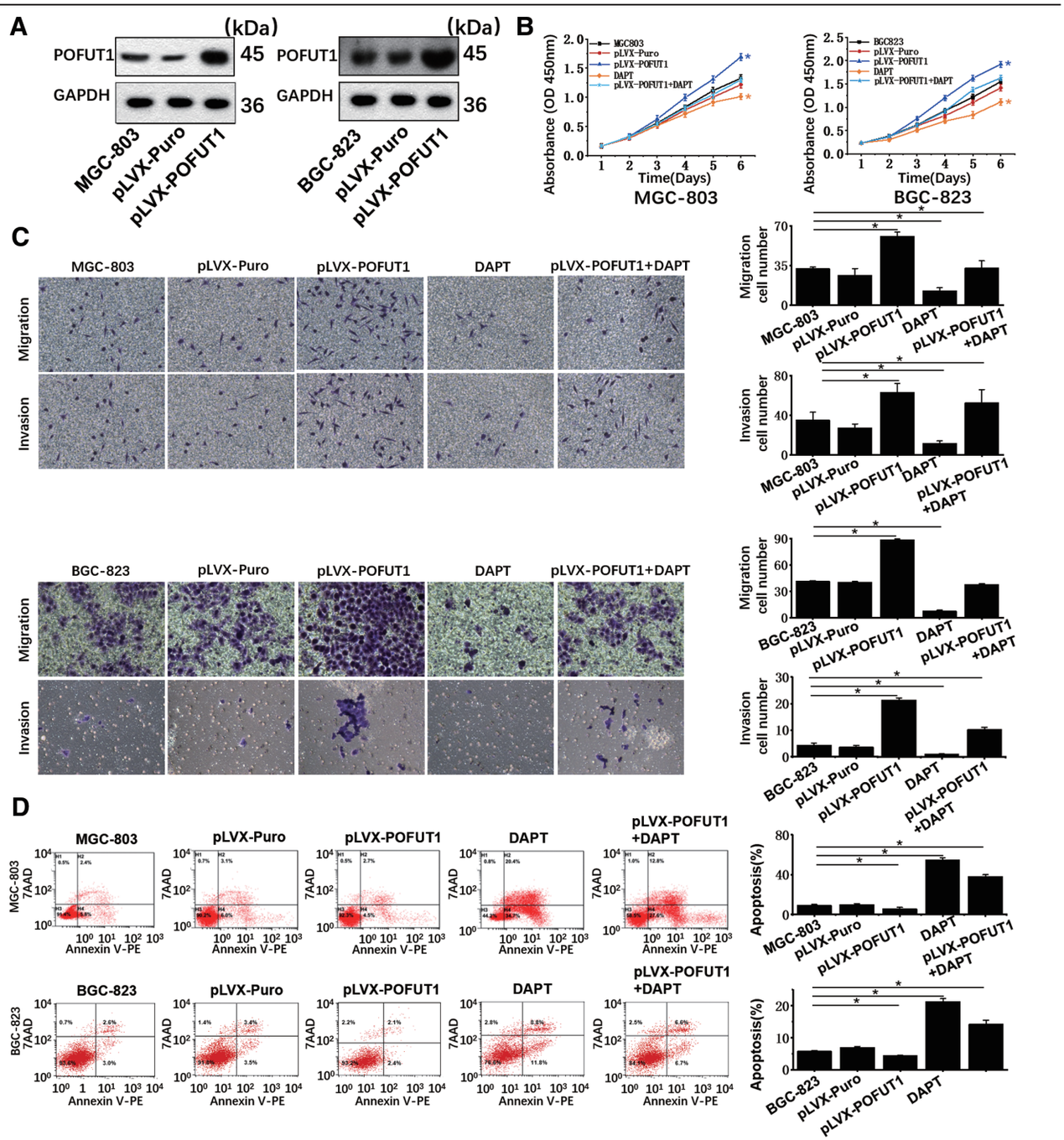

Fig. 2 The effects of POFUT1 overexpression and DAPT incubation in GC cells. A, POFUT1 protein levels in MGC-803 and BGC-823 cells with or without pLVX-Puro vector and pLVX-POFUT1 lentiviral vector. POFUT1 overexpression efficiency was confirmed using western blotting. B, Cell growth curves of MGC-803 (left panel; dark blue line: $p = 0.008$; orange line: $p = 0.042$) and BGC-823 cells (right panel; dark blue line: $p = 0.018$; orange line: $p = 0.002$). For pLVX-POFUT1 + DAPT compared with DAPT group: $p = 0.023$ (left panel) and $p = 0.011$ (right panel). C, Cell migration and invasion results of POFUT1-upregulated MGC-803 (two top panels; first bar chart *$p = 0.001$, $p = 0.004$, and $p = 0.015$ in sequence; second bar chart *$p = 0.001$, $p = 0.021$, and $p = 0.027$ in sequence) and BGC-823 cells (two bottom panels: first bar chart *$p = 0.003$ and $p = 0.004$; second bar chart *$p < 0.001$, $p = 0.013$, and $p = 0.002$ in sequence) using transwell assays. Representative images of the penetrated cells are shown. Magnification: ×100. D, Cell apoptosis analysis of POFUT1-upregulated and DAPT-treated MGC-803 (top panel; *$p = 0.01$, $p = 0.012$, and $p = 0.007$ in sequence) and BGC-823 (bottom panel; *$p = 0.002$, $p = 0.014$, and $p = 0.011$ in sequence) cells using flow cytometry. Results are shown as the mean ± SD based on triplicate experiments using a bar graph. *$p < 0.05$ vs vector control. BGC-823, MGC-803 = human gastric cancer cell lines; 7-AAD = 7-Aminoactinomycin D; annexin V-PE = annexin V-PE apoptosis detection kit; DAPT = N-[N-(3, 5-difluorophenacetyl)-l-alanyl]-s-phenylglycinet-butyl ester; GAPDH = glyceraldehyde-3-phosphate dehydrogenase; GC = gastric cancer; OD = optical density; POFUT1 = protein O-fucosyltransferase 1; pLVX-Puro = cells infected with pLVX-Puro vector.

3.3. The effects of POFUT1 on GC growth in vivo

To determine whether an aberrant POFUT1 expression affects GC growth in vivo, subcutaneous xenograft tumor models were established in nude mice using BGC-823 cells. We stably transfected BGC-823 cells with lentiviral particles carrying fluorescent shNC as a control and shPOFUT1-2 and injected

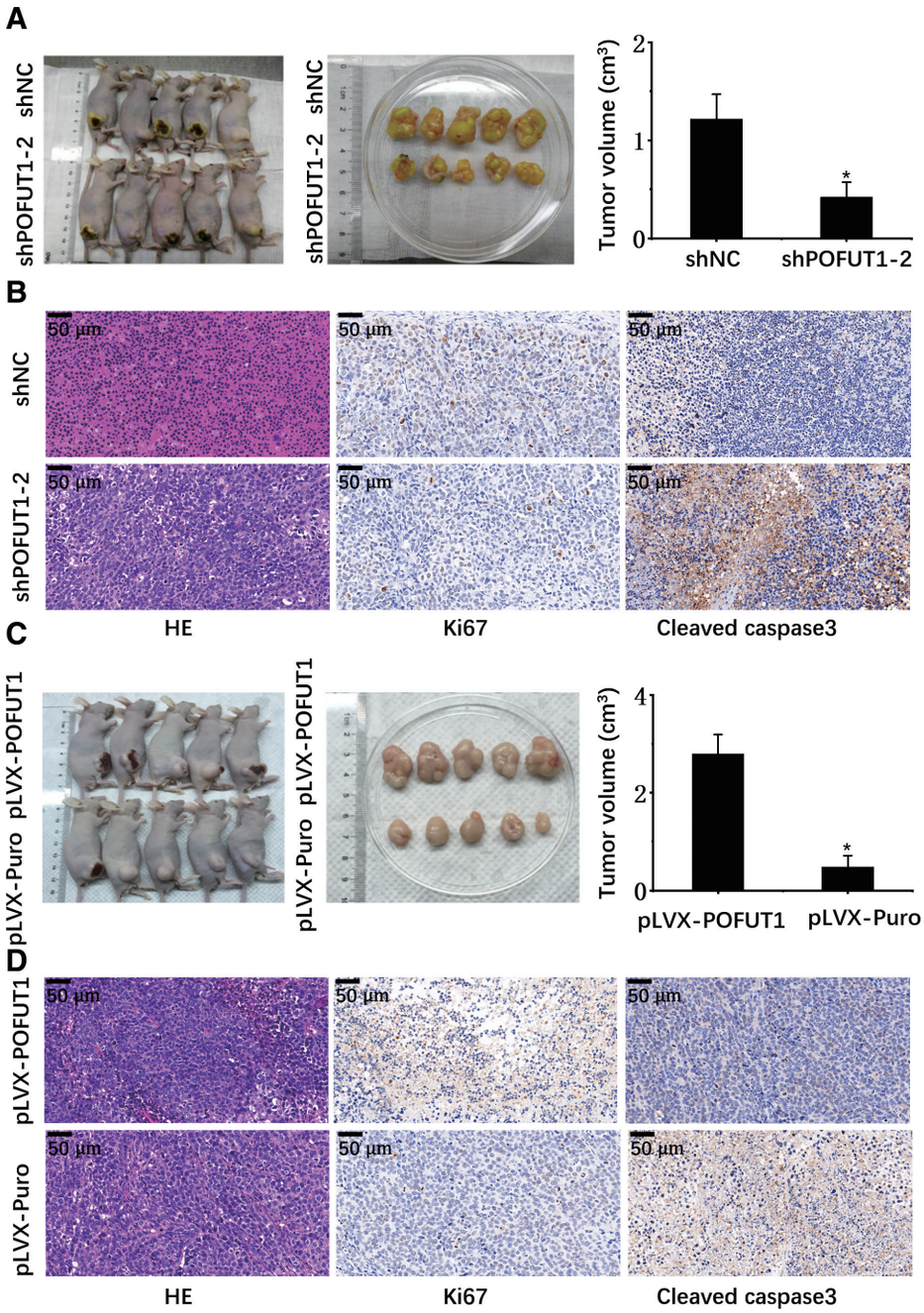

Fig. 3 The effects of regulating POFUT1 expression in vivo. A, Effects of POFUT1 silencing on tumor growth in subcutaneous xenograft tumor models. Left panel: representative images of BGC-823 xenograft tumors; middle panel: analysis of resected tumor volume; right panel: analysis of tumor volume in two groups (*p = 0.02). B, HE and IHC staining of Ki67 and cleaved caspase 3 representative photograph of resected tumors. Magnification: ×40 (scale: 50 μm). C, Effects of POFUT1 overexpression on tumor growth in subcutaneous xenograft tumor models. Left panel: representative images of BGC-823 xenograft tumors; middle panel: analysis of resected tumor volume; right panel: analysis of tumor volume in two groups (*p < 0.001). D, HE staining and IHC staining of Ki67 and cleaved caspase 3 with representative photographs of resected tumors. Magnification: ×40 (scale: 50 μm). Results are shown as the mean ± SD based on triplicate experiments using a bar graph. *p < 0.05 vs vector control. BGC-823 = human gastric cancer cell line; HE = hematoxylin-eosin; IHC = immunohistochemistry; POFUT1 = protein O-fucosyltransferase 1; shNC = lentivirus containing scramble nonsense control shRNA; shPOFUT1 = lentivirus containing short hairpin RNAs (shRNA) targeting POFUT1.

them into nude mice. All cell groups started to form measurable tumors at the primary implantation sites 1 week later. The transplanted tumor was resected surgically after 6 weeks. In concordance with the in vitro observations, there was a significant decrease in tumor growth in shPOFUT1-2 tumors (tumor size, 0.42 ± 0.15 cm^3) compared to control tumors (tumor size, 1.22 ± 0.31 cm^3) (Fig. 3A). Hematoxylin and eosin (H&E) staining and IHC were performed (Fig. 3B). The positive expression of Ki67 was localized in the nucleus of tumor cells stained with a buffy or dark brown color, while the positive expression of cleaved caspase 3 was localized in mainly the plasma but also the nucleus. IHC analysis showed a decreased Ki67 expression

and an increased cleaved caspase 3 expression in the shPOFUT1-2 group compared to that in the control group.

Moreover, BGC-823 cells stably transfected with lentivirus vector (pLVX-Puro) and POFUT1 overexpression vector (pLVX-POFUT1) were injected into nude mice and then monitored for tumor growth. After measurement, the mice injected with pLVX-POFUT1 clearly exhibited a significantly augmented tumor burden (tumor size, $2.79 \pm 0.58\,cm^3$) relative to those injected with pLVX-Puro (Fig. 3C, tumor size, $0.48 \pm 0.22\,cm^3$). IHC analysis showed that the tumors resected from pLVX-POFUT1 shared an increased Ki67 expression and a reduced cleaved caspase 3 expression compared to those in the pLVX-Puro group (Fig. 3D).

3.4. Driving factors of POFUT1 facilitate GC development

Our early bioinformatics analysis of GC specimens revealed that POFUT1 expression had a positive correlation with the cell cycle process, cell carcinoma, and Wnt signaling pathway, whereas it was negatively correlated with apoptosis and cell adhesion.[18] To investigate the reason underlying the carcinogenesis of POFUT1, the related proteins were assessed in POFUT1-silenced and overexpressed cells, as well as in DAPT-treated MGC-803 and BGC-823 cells. POFUT1 knockdown significantly decreased the expression of NICD1 and *hairy and enhancer of split homolog-1* (HES1) protein compared to that in control and shNC cells, as detected using western blotting. Furthermore, POFUT1-overexpressed GC cells showed a clear increase in the expression of NICD1 and HES1 compared to that in control and vector-transfected cells. DAPT-treated GC cells with and without POFUT1 upregulation exhibited a lower NICD1 and HES1 expression relative to vector-transfected and POFUT1-upregulated cells (Fig. 4A, B). Further explorations indicated that Cyclin D3 expression was positively correlated with POFUT1 expression and DAPT treatment alleviated Cyclin D3 expression in GC cells. Regarding the migration and invasion-related proteins, POFUT1 expression was positively correlated with MMP3 and MMP7 expression and negatively correlated with E-cadherin expression (Fig. 4A, B). The study of apoptotic proteins revealed that POFUT1 deficiency promoted Bax and cleaved caspase 3 expression, whereas POFUT1 upregulation inhibited Bax and cleaved caspase 3 expression. In addition, DAPT reversed the expression of Cyclin D3, MMP3, MMP7, E-cadherin, Bax, and cleaved caspase 3 independently of POFUT1 upregulation (Fig. 4A, B).

Moreover, the expression of β-catenin and phospho-β-catenin (Ser33/37/Thr41) were investigated in MGC-803 and BGC-823 cells. POFUT1-knockdown cells showed a decreased β-catenin expression but an increased β-catenin phosphorylation compared to control and shNC cells. In contrast, the upregulation of POFUT1 promoted β-catenin and inhibited β-catenin phosphorylation compared to that in control and vector-transfected cells. DAPT-treated GC cells with and without a POFUT1 overexpression inhibited β-catenin and promoted β-catenin phosphorylation relative to vector-transfected and cells with a POFUT1 upregulation (Fig. 4A, B). In addition, immunofluorescence confocal analysis showed that NICD1 and β-catenin expression are consistent with POFUT1 expression regulation. The increased cellular location of NICD1 and β-catenin indicated enhancive nuclear translocation, which was observed in POFUT1-upregulated cells. In addition, DAPT exerted a negative regulatory role against POFUT1 overexpression (Fig. 4C, D).

RBP-J is a Notch specific transcription factor; therefore, Notch signals in GC cells were assessed using an RBP-J-dependent luciferase reporter gene (pGL3-RBP-J) assay. The luciferase reporter assay results suggested that the RBP-J luciferase activity in POFUT1-knockdown cells was lower than that in control and negative cells. RBP-J luciferase activity in cells with a POFUT1 overexpression was higher than in control and vector-transfected cells. DAPT treatment inhibited RBP-J luciferase activity (Fig. 4E). In addition, when the Wnt signal is active, the engagement of β-catenin transiently converts TCF into a transcriptional activator.[21] Therefore, the plasmid pGL3-TCF was constructed and GC cells were transfected with pGL3 luciferase reporter plasmids. The results of the dual luciferase reporter assay showed that a low TCF luciferase activity was observed in POFUT1 knockdown cells, while a high TCF luciferase activity was observed in POFUT1 upregulated cells. DAPT weakened the TCF luciferase activity against POFUT1-upregulation (Fig. 4F). Similar results were observed in MGC-803 and BGC-823 cells. All these data indicate that POFUT1 is involved in Notch and Wnt signaling activation.

3.5. Carcinogenesis of POFUT1 is regulated both by Notch and Wnt signaling pathways

Understanding of the regulatory effect of Notch and Wnt signaling in POFUT1-overexpressed GC cells is limited. To address this issue, Flag-NICD1 and shβ-catenin plasmids were constructed and stably transfected into BGC-823 cells. BGC-823 cells were divided into six treatment groups: pLVX-Puro (negative control), pLVX-POFUT1, Flag-NICD1, shβ-catenin, pLVX-POFUT1 and shβ-catenin co-transfection, and Flag-NICD1 and shβ-catenin co-transfection. Cell proliferation, migration, invasive ability, and the apoptosis rate were then studied. CCK8 assay showed that POFUT1- and NICD1-overexpressed cells showed higher cell growth compared to the negative control. However, β-catenin silencing inhibited cell growth in POFUT1- and NICD1-overexpressed cells (Fig. 5A). The results of the migration and invasion assays showed a similar trend to those of the CCK8 assay (Fig. 5B). Moreover, POFUT1 and NICD1 overexpression inhibited cell apoptosis, and β-catenin knockdown promoted cell apoptosis in untreated cells, as well as in POFUT1- and NICD1-overexpressed cells (Fig. 5C). To further study the involvement of the related proteins, the expression of regulatory proteins was assessed using western blotting in the cells treated as described above. POFUT1 and NICD1 upregulation promoted the expression of HES1, Cyclin D3, MMP3, MMP7, and β-catenin, while they inhibited the expression of E-cadherin, Bax, cleaved caspase 3, and phosphorylated β-catenin. Nevertheless, β-catenin knockdown exerted opposite effects in untreated cells, as well as in POFUT1- and NICD1-overexpressed cells (Fig. 5D; Fig. S1, http://links.lww.com/JCMA/A199).

The activity of RBP-J and TCF luciferase was used to evaluate the activation of Notch and Wnt signaling in pGL3-RBP-J- and pGL3-TCF-transfected cells. As expected, RBP-J luciferase activity was increased in POFUT1- and NICD1-overexpressed cells compared to the negative control, whereas no clear changes in β-catenin-silenced cells alone were observed (Fig. 5E). TCF luciferase activity was also increased significantly when POFUT1 and NICD1 were overexpressed. In addition, β-catenin knockdown impaired the TCF luciferase activity although POFUT1 and NICD1 were overexpressed (Fig. 5F). These observations indicated that the carcinogenesis of POFUT1 depends on Notch and Wnt signaling activation simultaneously.

3.6. POFUT1 regulates the parafibromin-NICD1-β-catenin complex in GC pathogenesis

POFUT1 functions were restricted to Notch signaling; thus, the crosstalk between Notch and Wnt signaling was further investigated. It was assumed that the coactivator of Notch and Wnt signaling might be NICD1 itself or other downstream factors. To examine the interaction between NICD1 and β-catenin, a co-immunoprecipitation study was performed using BGC-823 cells

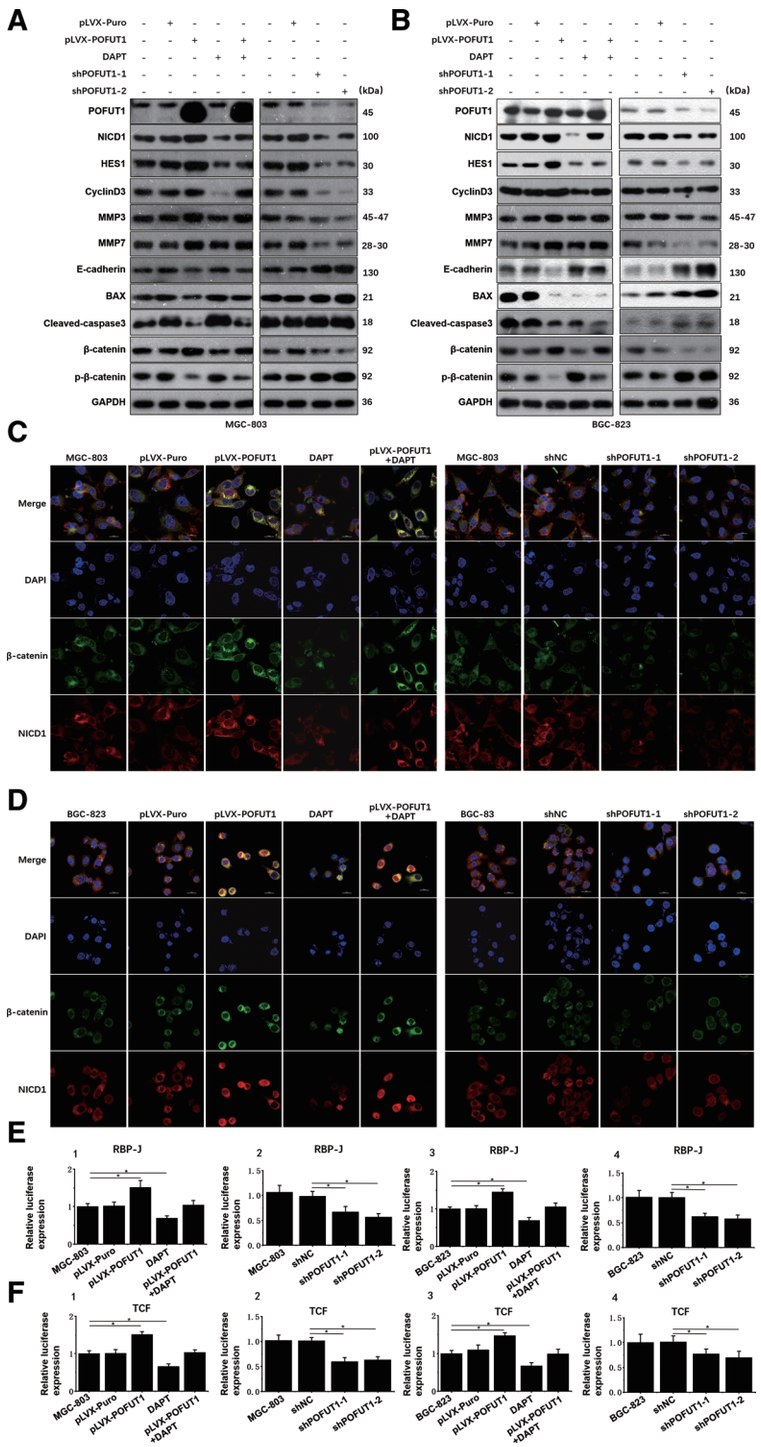

Fig. 4 The expression of related proteins and transcription factors involved in POFUT1 expression regulation. A, The level of related proteins in MGC-803 cells assessed using western blotting. B, The level of related proteins in BGC-823 cells assessed using western blotting. C, Immunofluorescence staining of DAPI (blue), β-catenin (green), and NICD1 (red) in MGC-803 cells. Magnification: ×800 (scale: 20 μm). D, Immunofluorescence staining of DAPI (blue), β-catenin (green), and NICD1 (red) in BGC-823 cells. Magnification: ×800 (scale: 20 μm). E, Transactivation of pGL3-RBP-J assessed using a dual luciferase reporter assay in MGC-803 and BGC-823 cells. E1: $p = 0.0030$, $p = 0.0358$; E2: $p = 0.0161$, $p = 0.0034$; E3: $p = 0.0003$, $p = 0.0032$; E4: $p = 0.0036$, $p = 0.0018$. F, Transactivation of pGL3-TCF assessed using a dual luciferase reporter assay in MGC-803 and BGC-823 cells. F1: $p < 0.001$, $p = 0.0020$; F2: $p = 0.0419$, $p = 0.0382$; F3: $p = 0.0057$, $p = 0.0033$; F4: $p = 0.0469$, $p = 0.0053$. Results are shown as mean ± SD based on triplicates experiments using a bar graph. $^*p < 0.05$ vs vector control. BGC-823, MGC-803 = human gastric cancer cell lines; BAX = Bcl-2-associated X protein; DAPI = 4',6-diamidino-2-phenylindole; DAPT = N-[N-(3, 5-difluorophenacetyl)-l-alanyl]-s-phenylglycinet-butyl ester; GAPDH = glyceraldehyde-3-phosphate dehydrogenase; HES-1 = hairy and enhancer of split homolog-1; MMP = matrix metalloproteinase; NICD1 = Notch1 intracellular domain; pGL3 = luciferase reporter vector; pLVX-Puro = cells infected with pLVX-Puro vector; POFUT1 = protein O-fucosyltransferase 1; RBP-J = recombination signal binding protein-Jκ; shNC = lentivirus containing scramble nonsense control shRNA; shPOFUT1 = lentivirus containing short hairpin RNAs (shRNA) targeting POFUT1; TCF = T-cell factor.

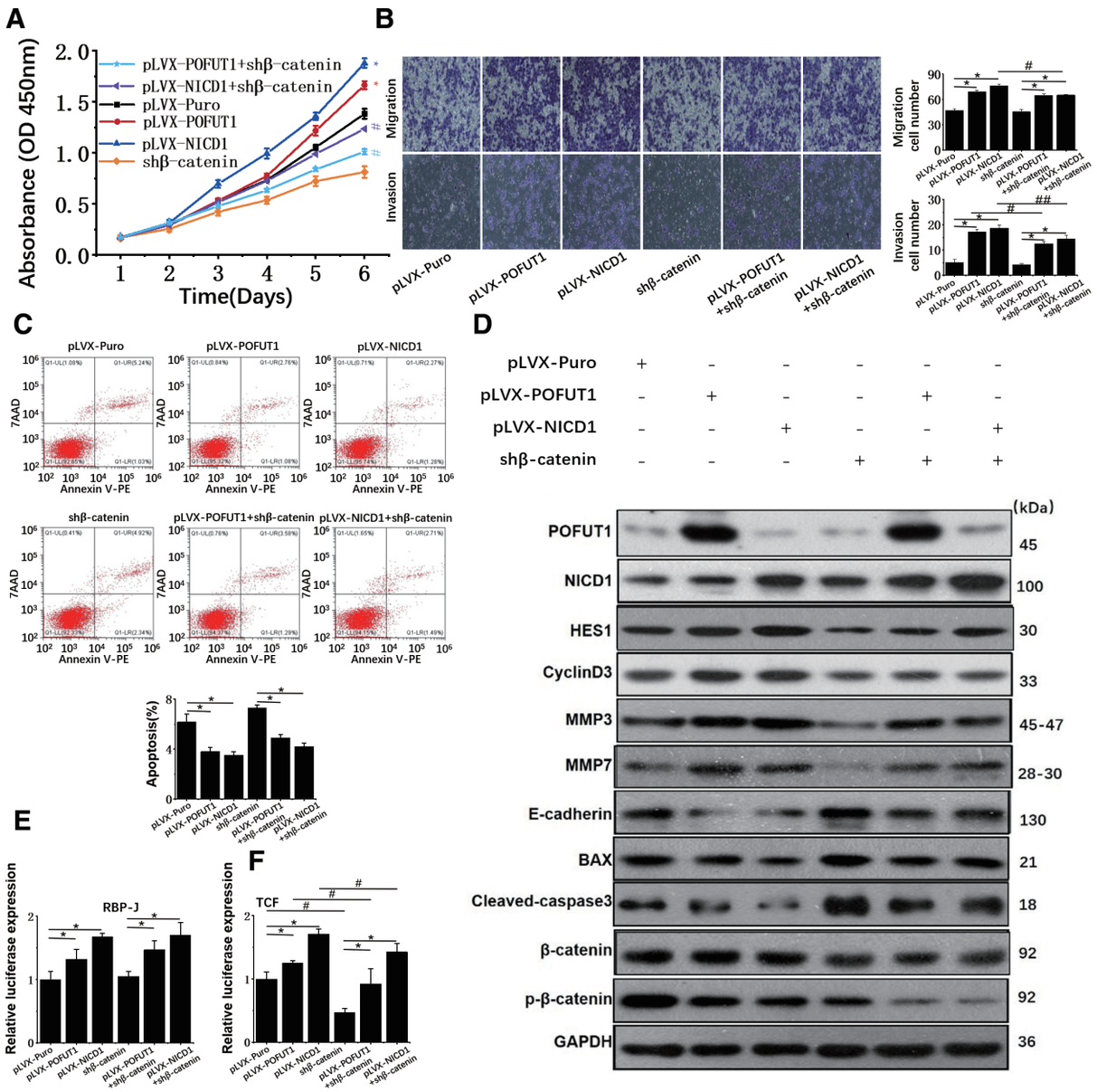

Fig. 5 POFUT1 exerts carcinogenesis through Notch/Wnt dual signaling pathways. A, Cell growth curves of BGC-823 cells tested using a CCK8 assay (dark $^{*}p = 0.0021$; red $^{*}p = 0.0031$; purple $\#p = 0.0024$; light blue $^{*}p = 0.0052$). B, Cell migration (top panel: $^{*}p < 0.001$; $\#p = 0.001$) and invasion (bottom panel: $^{*}p < 0.001$; $\#p = 0.008$; $\#\#p = 0.037$) results detected using transwell assays. Representative images of penetrated cells are shown. Magnification: ×100. C, Cell apoptosis analysis using a flow cytometry assay. $^{*}p = 0.0132$, $p = 0.0028$, $p = 0.0034$, and $p = 0.0035$ in sequence. D, The expression level of related proteins assessed using western blotting. E, Transactivation of pGL3-RBP-J assessed using a dual luciferase reporter assay ($^{*}p < 0.001$). F, Transactivation of pGL3-TCF assessed using a dual luciferase reporter assay ($^{*}p < 0.001$; $\#p = 0.0023$, $p = 0.0078$, $p < 0.001$ in sequence). Results are shown at the mean ± SD based on triplicate experiments using a bar graph. $^{*}p < 0.05$, $\#p < 0.05$. 7-AAD = 7-Aminoactinomycin D; annexin V-PE = annexin V-PE apoptosis detection kit; BAX = Bcl-2-associated X protein; BGC-823 = human gastric cancer cell line; CCK8 = cell counting Kit-8; GAPDH = glyceraldehyde-3-phosphate dehydrogenase; HES-1 = hairy and enhancer of split homolog-1; MMP: matrix metalloproteinase; NICD1 = Notch1 intracellular domain; OD = optical density; POFUT1 = protein O-fucosyltransferase 1; pGL3 = luciferase reporter vector; pLVX-Puro = cells infected with pLVX-Puro vector; RBP-J = recombination signal binding protein-Jκ; shβ-catenin = lentivirus containing short hairpin RNAs (shRNA) targeting β-catenin; TCF = T-cell factor.

transfected with Flag-NICD1 and HA-β-catenin plasmids. As shown in Fig. 6A, NICD1 did not co-precipitate with β-catenin, indicating that NICD1 did not directly interact with β-catenin.

To gain further insight into its possible coactivator, the Myc-parafibromin plasmid and the constitutively active β-catenin S33Y mutant, which is insensitive to glycogen synthase kinase-3β (GSK-3β)–mediated phosphorylation and proteasomal degradation, were constructed. BGC-823 cells were simultaneously transfected with Flag-NICD1, HA-β-catenin S33Y, Myc-parafibromin, and shPOFUT1. NICD1 and parafibromin from triple-transfected cells co-immunoprecipitated with β-catenin. Furthermore, the parafibromin-NICD1-β-catenin heterotrimeric complex was impaired when POFUT1 was knocked down (Fig. 6B). These results indicated that parafibromin integrated NICD1 and β-catenin, thereby supporting the concerted activation of Notch and Wnt signaling. POFUT1 regulated the

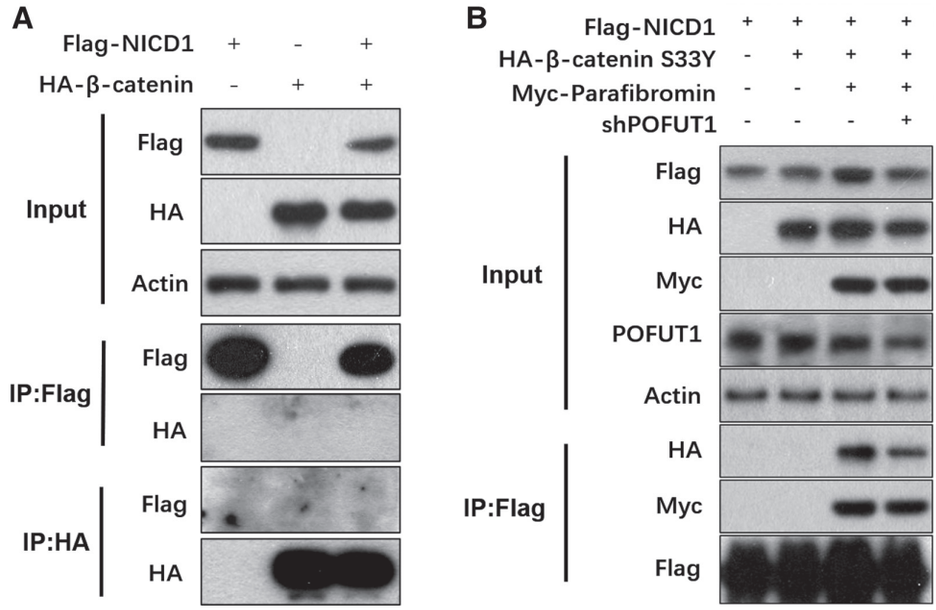

Fig. 6 Identification of coactivator of Notch and Wnt signaling. A, NICD1 and β-catenin immunoprecipitation from BGC-823 cells. B, Parafibromin and NICD1, as well as β-catenin immunoprecipitation from BGC-823 cells transfected with or without POFUT1 knockdown. Experiments were performed in triplicates and representative images are shown above. BGC-823 = human gastric cancer cell line; HA = hemagglutinin tag; IP = immunoprecipitation; Myc = Myc-tag; NICD1 = Notch1 intracellular domain; POFUT1 = protein O-fucosyltransferase 1; shPOFUT1 = lentivirus containing short hairpin RNAs (shRNA) targeting POFUT1.

parafibromin-NICD1-β-catenin complex, which provided evidence to GC progression.

4. DISCUSSION

Glycosylation performed by GTs is a crucial cellular mechanism that is often altered in several types of diseases. An aberrant GT expression leads to altered glycosylation patterns, contributing to cancer progression. Fucosylation is a type of cancer-related glycosylation that includes core fucosylation and O-fucosylation. POFUT1, a member of the fucosyltransferase (FUT) family, participates in O-fucosylation of EGF repeats found on up to 100 different targets in mammals, including Notch receptors and their ligands.[22] It has been reported that in Notch proteins, Ser and Thr residues between the second and third Cys residues within EGF domains are modified by the addition of O-Fuc by POFUT1.[23,24] Then, the Fuc residue can be extended by additional GTs to form the tetrasaccharide SA-α2,6-Gal-β1,4-GlcNAc-β1,3-Fuc-α1-O-Ser.[25] The influence of POFUT1 on Notch activation can be positive or negative, depending on the POFUT1 expression level and on whether the signal to Notch comes from Delta or γ-Serrate.[26] Early studies by our group have demonstrated that POFUT1 is overexpressed in human GC specimens and significantly correlates with T and N classification, as well as with tumor differentiation. However, little is known about the function and mechanism of POFUT1 in GC development. In this study, we investigated the biological effects and the regulation mechanism of POFUT1 both in vitro and in vivo, as well as the involved downstream signaling pathways.

A high POFUT1 expression was observed in six GC cells to different degrees. Functionally, the oncogenic phenotypes of GC cell lines were dependent on POFUT1 expression and were attenuated by γ-secretase inhibitor DAPT treatment. POFUT1 knockdown showed reduced proliferation and metastasis, and an enhanced apoptosis rate in MGC-803 and BGC-823 cell lines. However, POFUT1 upregulation resulted in opposite phenotypes. In line with the in vitro findings, POFUT1 was observed to promote GC tumor formation in vivo using subcutaneous xenograft tumor models in nude mice. In terms of the related mechanisms, the results indicated that POFUT1 expression was positively correlated with Cyclin D3 expression, which drives cell proliferation,[27] and negatively correlated with the expression of apoptotic proteins, such as Bax and cleaved caspase 3. POFUT1 promoted the expression of MMP3 and MMP7 and inhibited the expression of E-cadherin, which results in a pro-metastasis effect in GC. In contrast, DAPT reversed the expression of Cyclin D3, MMP3, MMP7, E-cadherin, Bax, and cleaved caspase 3 even when POFUT1 was upregulated. Notably, POFUT1 overexpression promoted Notch and Wnt signaling target genes and enhanced luciferase activity of transcription factor RBP-J and TCF, which resulted in upregulated NICD1 and β-catenin nuclear translocation. Furthermore, consistent with POFUT1 overexpression, NICD1 overexpression in GC cells showed pro-oncogenic effects and stimulated the same expression of downstream target factors. In addition, β-catenin knockdown inhibited both the oncogenic effects of POFUT1 and NICD1 upregulation. Notably, expression of HES1, a downstream target molecule of NICD1, depended on NICD1 expression even when β-catenin was knocked down. Commonly, dephosphorylated β-catenin promotes the accumulation of β-catenin in the cytoplasm and nucleus, which may trigger Wnt signaling. When β-catenin was knocked down, phosphorylated β-catenin showed a clear reduction accompanied by decreased β-catenin. These observations indicated that the carcinogenesis of POFUT1 depended on the simultaneous Notch and Wnt signaling activation.

Notch and Wnt signaling pathways are highly conserved cell-fate-determination pathways that participate in organ development, tissue homeostasis, and multiple aspects of cancer biology.[28,29] Notch signal transduction relies on ligand-receptor binding, which allows Notch to undergo sequential proteolytic cleavage, and is mediated by the γ-secretase

complex to release NICD1.[30] NICD1 then translocates into the nucleus and behaves as a transcriptional regulator in complex with DNA-binding RBP-J protein. As a result, the expression of related target genes is induced, including the *hairy and enhancer of split* (*HES*) *1–7* and *HES-related repressor* (*HEY*) *1,2*.[31] As for the canonical Wnt signaling, Wnt ligand binding to Frizzled (Fz)/low-density lipoprotein-related protein (LRP) co-receptors inhibits β-catenin turnover, leading to the activation of β-catenin/TCF-dependent transcription and target genes.[32,33]

Notch/Wnt dual signaling is triggered simultaneously and shaped intracellularly to generate appropriate cellular responses in GC. However, it is still unknown whether they work independently or cooperatively in GC. The crosstalk between Notch and Wnt dual signaling was therefore further investigated. In addition to ligand/receptor binding and cross-regulation at the cytoplasmic signal transducer level, a signal effector that integrates multiple signals and is converted to generate an output was explored. It was assumed that the coactivator of Notch and Wnt signaling might be NICD1 or other downstream factors. Since it has been demonstrated that NICD1 does not coprecipitate with β-catenin, attention has been paid to the interaction between NICD1 and parafibromin, which is a component of the polymerase-associated factor 1 (PAF1) complex. Parafibromin binds to NICD and stabilizes NICD by inhibiting proteasome-dependent degradation. The complex formed by parafibromin and NICD depends on the tyrosine dephosphorylation of parafibromin, which shows more potential in activating Notch signaling than wild-type parafibromin.[34] It has also been reported that parafibromin is also involved in activating Wnt target gene transcription via direct association with β-catenin,[35] which is potentiated by tyrosine dephosphorylation at the Y290/293/315 of parafibromin.[36] In order to examine the effect of parafibromin in GC, co-immunoprecipitation was performed and indicated that parafibromin stabilized the NICD1/β-catenin interaction. More importantly, the parafibromin-NICD1-β-catenin complex was impaired in the presence of POFUT1 knockdown. Mechanistically, POFUT1 stimulated the Notch/Wnt dual signaling pathways by forming the parafibromin-NICD1-β-catenin complex.

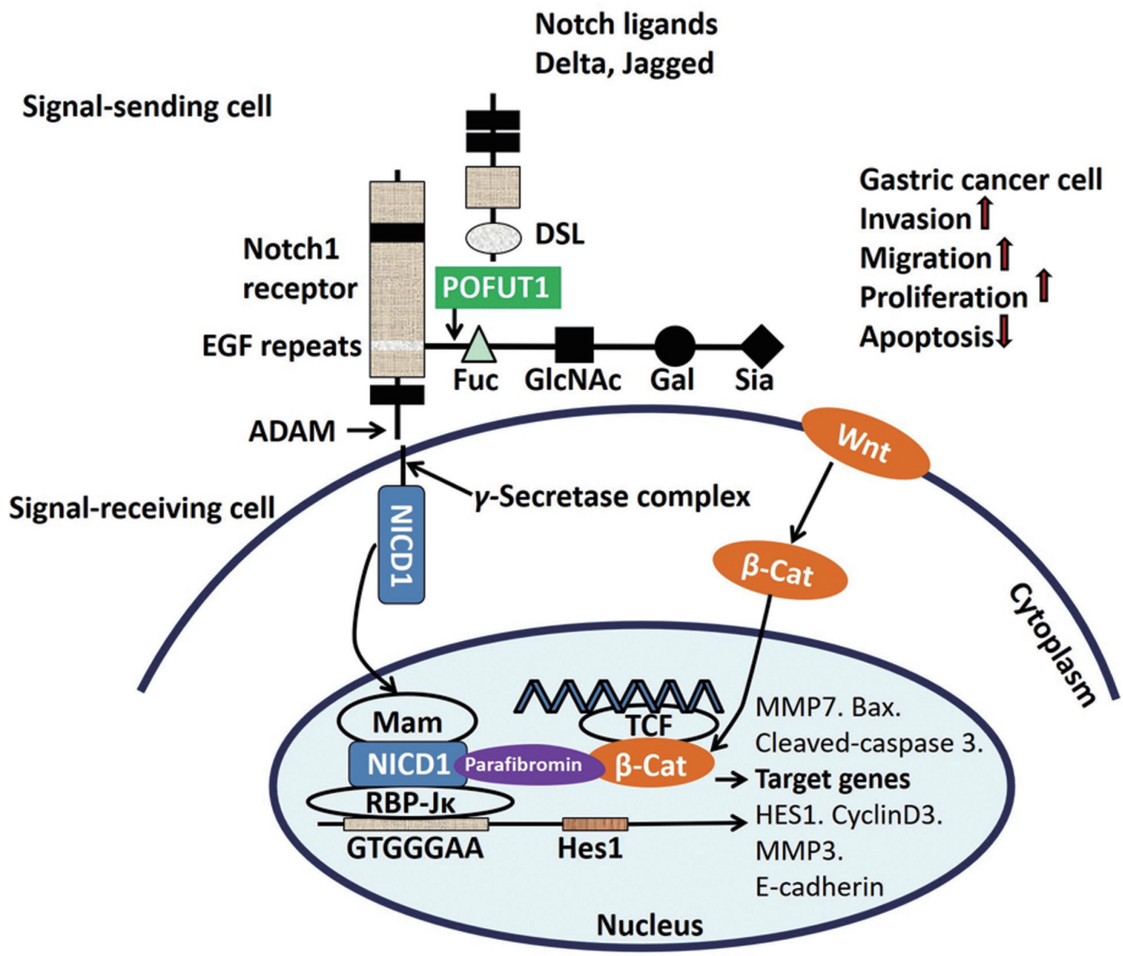

Fig. 7 Schematic. POFUT1, participating in O-fucosylation of EGF repeats on NICD1, activates Notch/Wnt dual signaling pathways, enhances GC cell proliferation and metastasis, and inhibits apoptosis in GC development. The specific process is as follows: the upregulation of NICD1 modified by POFUT1 promotes RBP-J transcription to activate Notch signaling. Meanwhile, NICD1 is involved in the formation of the parafibromin-NICD1-β-catenin complex, which enhances β-catenin nuclear translocation and inhibits β-catenin phosphorylation degradation. Ultimately, TCF transcription is increased to activate the Wnt signaling pathway. β-Cat = β-catenin; ADAM = a disintegrin and metalloprotease; DSL = a conserved cysteine-rich region found in the Delta/Serrate/Lag2; EGF = epidermal growth factor; Fuc = fucose; Gal = galactose; GlcNAc = N-acetylglucosamine; GC = gastric cancer; GTGGGAA = a sequence that is recognized by RBP-J; HES1 = hairy and enhancer of split homolog-1; Mam = mastermind; MMP = matrix metalloproteinase; NICD1 = Notch1 intracellular domain; POFUT1 = protein O-fucosyltransferase 1; RBP-J = recombination signal binding protein-Jκ; Sia = sialic acid; TCF = T-cell factor.

Collectively, POFUT1 is in charge of the O-fucosylation of EGF repeats on NICD1, which promotes Notch and Wnt target protein expression, thereby activating Notch/Wnt dual signaling simultaneously in GC. POFUT1 plays a pro-oncogenic role both in vivo and in vitro, which promotes GC cell proliferation and metastasis and inhibits apoptosis. The specific process is as follows: the upregulation of NICD1 modified by POFUT1 promotes RBP-J transcription to activate Notch signaling. Meanwhile, NICD1 is involved in the formation of the parafibromin-NICD1-β-catenin complex, which enables the concerted activation of Notch and Wnt target genes. Accumulated β-catenin regulated by POFUT1 is transported to the nucleus, accompanied by a reduced β-catenin phosphorylation degradation. Ultimately, TCF transcription is increased to activate the Wnt signaling pathway (a schematic diagram is shown in Fig. 7). This study reveals the regulation effect and related mechanism of POFUT1 in GC progression for the first time, which provides new evidence for GC diagnosis and treatment. The potential value of POFUT1 may be associated with a quick lectin assay for detection and effective inhibition of drug targets in the future.

ACKNOWLEDGMENTS

This study was supported by the fund of Pudong New Area Clinical Characteristic Discipline Project (PWYts2021-11).

APPENDIX A. SUPPLEMENTARY DATA

Supplementary data related to this article can be found at http://links.lww.com/JCMA/A199.

REFERENCES

1. Torre LA, Bray F, Siegel RL, Ferlay J, Lortet-Tieulent J, Jemal A. Global cancer statistics, 2012. *CA Cancer J Clin* 2015;**65**:87–108.
2. Zhang XY, Zhang PY. Gastric cancer: somatic genetics as a guide to therapy. *J Med Genet* 2017;**54**:305–12.
3. Ferreira JA, Magalhaes A, Gomes J, Peixoto A, Gaiteiro C, Fernandes E, et al. Protein glycosylation in gastric and colorectal cancers: toward cancer detection and targeted therapeutics. *Cancer Lett* 2017;**387**:32–45.
4. Miyoshi E, Moriwaki K, Nakagawa T. Biological function of fucosylation in cancer biology. *J Biochem* 2008;**143**:725–9.
5. Haltom AR, Jafar-Nejad H. The multiple roles of epidermal growth factor repeat O-glycans in animal development. *Glycobiology* 2015;**25**:1027–42.
6. Vasudevan D, Takeuchi H, Johar SS, Majerus E, Haltiwanger RS. Peters plus syndrome mutations disrupt a noncanonical ER quality-control mechanism. *Curr Biol* 2015;**25**:286–95.
7. Takeuchi H, Yu HJ, Hao HL, Takeuchi M, Ito A, Li HL, et al. O-glycosylation modulates the stability of epidermal growth factor-like repeats and thereby regulates Notch trafficking. *J Biol Chem* 2017;**292**:15964–73.
8. Ishio A, Sasamura T, Ayukawa T, Kuroda J, Ishikawa HO, Aoyama N, et al. O-fucose monosaccharide of drosophila Notch has a temperature-sensitive function and cooperates with O-glucose glycan in Notch transport and Notch signaling activation. *J Biol Chem* 2015;**290**:505–19.
9. Yokota S, Ogawara K, Kimura R, Shimizu F, Baba T, Minakawa Y, et al. Protein O-fucosyltransferase 1: a potential diagnostic marker and therapeutic target for human oral cancer. *Int J Oncol* 2013;**43**:1864–70.
10. Ma LJ, Dong PP, Liu LZ, Gao Q, Duan M, Zhang S, et al. Overexpression of protein O-fucosyltransferase 1 accelerates hepatocellular carcinoma progression via the Notch signaling pathway. *Biochem Bioph Res Co* 2016;**473**:503–10.
11. Wan GX, Tian L, Yu YD, Li F, Wang XB, Li C, et al. Overexpression of Pofut1 and activated Notch1 may be associated with poor prognosis in breast cancer. *Biochem Bioph Res Co* 2017;**491**:104–11.
12. Leng QX, Tsou JH, Zhan M, Jiang F. Fucosylation genes as circulating biomarkers for lung cancer. *J Cancer Res Clin* 2018;**144**:2109–15.
13. Wang SC, Itoh M, Shiratori E, Ohtaka M, Tohda S. NOTCH activation promotes glycosyltransferase expression in human myeloid leukemia cells. *Hematol Rep* 2018;**10**:84–7.
14. Yao D, Huang YS, Huang XR, Wang WH, Yan QJ, Wei LB, et al. Protein O-fucosyltransferase 1 (Pofut1) regulates lymphoid and myeloid homeostasis through modulation of Notch receptor ligand interactions. *Blood* 2011;**117**:5652–62.
15. Takeuchi H, Wong D, Schneider M, Freeze HH, Takeuchi M, Berardinelli SJ, et al. Variant in human POFUT1 reduces enzymatic activity and likely causes a recessive microcephaly, global developmental delay with cardiac and vascular features. *Glycobiology* 2018;**28**:276–83.
16. McMillan BJ, Zimmerman B, Egan ED, Lofgren M, Xu X, Hesser A, et al. Structure of human POFUT1, its requirement in ligand-independent oncogenic Notch signaling, and functional effects of Dowling-Degos mutations. *Glycobiology* 2017;**27**:777–86.
17. Zhong W, Liu J, Wang H, Dou X, Yu B, Lin Z, et al. Atypical presentation of Dowling-Degos disease with novel and recurrent mutations in POFUT1. *Clin Exp Dermatol* 2018;**43**:937–9.
18. Dong S, Wang Z, Huang B, Zhang J, Ge Y, Fan Q, et al. Bioinformatics insight into glycosyltransferase gene expression in gastric cancer: POFUT1 is a potential biomarker. *Biochem Biophys Res Commun* 2017;**483**:171–7.
19. Fortini ME. Notch signaling: the core pathway and its posttranslational regulation. *Dev Cell* 2009;**16**:633–47.
20. Haseeb M, Pirzada RH, Ain QU, Choi S. Wnt signaling in the regulation of immune cell and cancer therapeutics. *Cells* 2019;**8**:1380.
21. Nusse R, Clevers H. Wnt/beta-catenin signaling, disease, and emerging therapeutic modalities. *Cell* 2017;**169**:985–99.
22. Zhang C, Huang H, Zhang J, Wu Q, Chen X, Huang T, et al. Caveolin-1 promotes invasion and metastasis by upregulating Pofut1 expression in mouse hepatocellular carcinoma. *Cell Death Dis* 2019;**10**:477.
23. Shao L, Moloney DJ, Haltiwanger R. Fringe modifies O-fucose on mouse Notch1 at epidermal growth factor-like repeats within the ligand-binding site and the Abruptex region. *J Biol Chem* 2003;**278**:7775–82.
24. Wang Y, Shao L, Shi S, Harris RJ, Spellman MW, Stanley P, et al. Modification of epidermal growth factor-like repeats with O-fucose. Molecular cloning and expression of a novel GDP-fucose protein O-fucosyltransferase. *J Biol Chem* 2001;**276**:40338–45.
25. Moremen KW, Tiemeyer M, Nairn AV. Vertebrate protein glycosylation: diversity, synthesis and function. *Nat Rev Mol Cell Biol* 2012;**13**:448–62.
26. Lei L, Xu A, Panin VM, Irvine KD. An O-fucose site in the ligand binding domain inhibits Notch activation. *Development* 2003;**130**:6411–21.
27. Sherr CJ, Beach D, Shapiro GI. Targeting CDK4 and CDK6: from discovery to therapy. *Cancer Discov* 2016;**6**:353–67.
28. Espinoza I, Miele L. Notch inhibitors for cancer treatment. *Pharmacol Ther* 2013;**139**:95–110.
29. Hayward P, Kalmar T, Arias AM. Wnt/Notch signalling and information processing during development. *Development* 2008;**135**:411–24.
30. Nagase H, Nakayama K. γ-Secretase-regulated signaling typified by Notch signaling in the immune system. *Curr Stem Cell Res Ther* 2013;**8**:341–56.
31. Yan M. Therapeutic promise and challenges of targeting DLL4/NOTCH1. *Vasc Cell* 2011;**3**:17.
32. Duchartre Y, Kim YM, Kahn M. The Wnt signaling pathway in cancer. *Crit Rev Oncol Hematol* 2016;**99**:141–9.
33. Freeman J, Smith D, Latinkic B, Ewan K, Samuel L, Zollo M, et al. A functional connectome: regulation of Wnt/TCF-dependent transcription by pairs of pathway activators. *Mol Cancer* 2015;**14**:206.
34. Kikuchi I, Takahashi-Kanemitsu A, Sakiyama N, Tang C, Tang PJ, Noda S, et al. Dephosphorylated parafibromin is a transcriptional coactivator of the Wnt/Hedgehog/Notch pathways. *Nat Commun* 2016;**7**:12887.
35. Mosimann C, Hausmann G, Basler K. Parafibromin/Hyrax activates Wnt/Wg target gene transcription by direct association with beta-catenin/Armadillo. *Cell* 2006;**125**:327–41.
36. Takahashi A, Tsutsumi R, Kikuchi I, Obuse C, Saito Y, Seidi A, et al. SHP2 tyrosine phosphatase converts parafibromin/Cdc73 from a tumor suppressor to an oncogenic driver. *Mol Cell* 2011;**43**:45–56.